Supporting Information

for

Soluble Salt Self-Assembly-Assisted Synthesis of Three-Dimensional Hierarchical Porous Carbon Networks for Supercapacitors

Shan Zhu [a], Jiajun Li [a], Chunnian He [a,b,*] , Naiqin Zhao [a,b,*], Enzuo Liu [a,b], Chunsheng Shi [a], Miao Zhang [a]

[a]*School of Materials Science and Engineering and Tianjin Key Laboratory of Composites and Functional Materials, Tianjin University, Tianjin 300072, China*

[b]*Collaborative Innovation Center of Chemical Science and Engineering, Tianjin 300072, China*

*Corresponding authors:

Tel: +086-13512958908

Email: cnhe08@tju.edu.cn (C. He), nqzhao@tju.edu.cn (N. Zhao)

Table S1. The composition of raw materials for producing target materials

Samples	Glucose [g]	NaCl [g]	Na_2CO_3 [g]	Na_2SiO_3 [g]
HPC-M	1.25	--	25	--
HPC-S	1.25	--	--	2
HPC-BM	1.25	20	0.5	--
HPC-MS	1.25	--	25	0.1
HPC-BS	1.25	20	--	0.4
HPC-BMS	1.25	20	0.5	0.5
CB	1.25	0	0	0

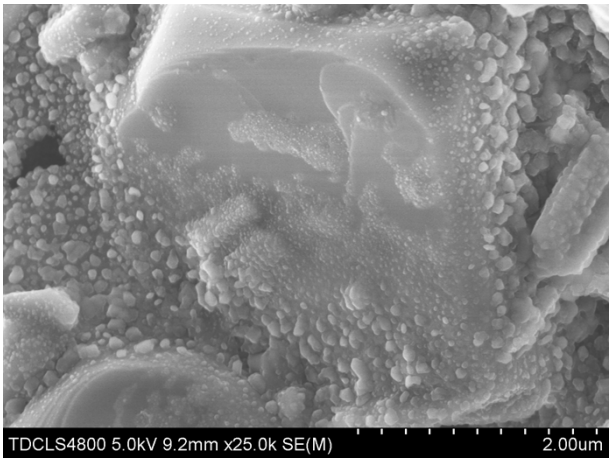

Fig. S1. SEM image of the calcined sample before washing, indicating the salt crystals with three kinds of length scales.

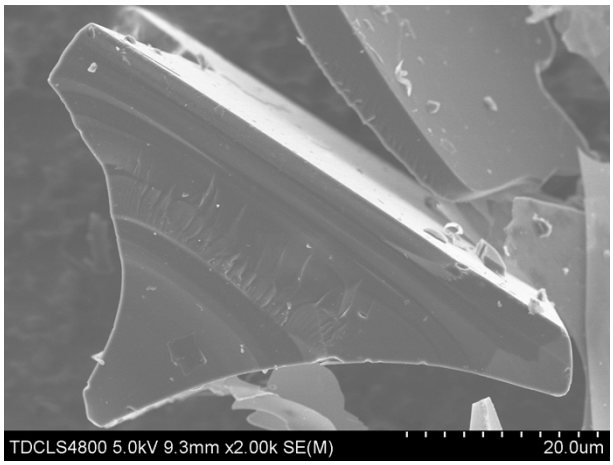

Fig. S2. SEM image of the carbon bulk (CB) fabricated without the assistance of salt templates.

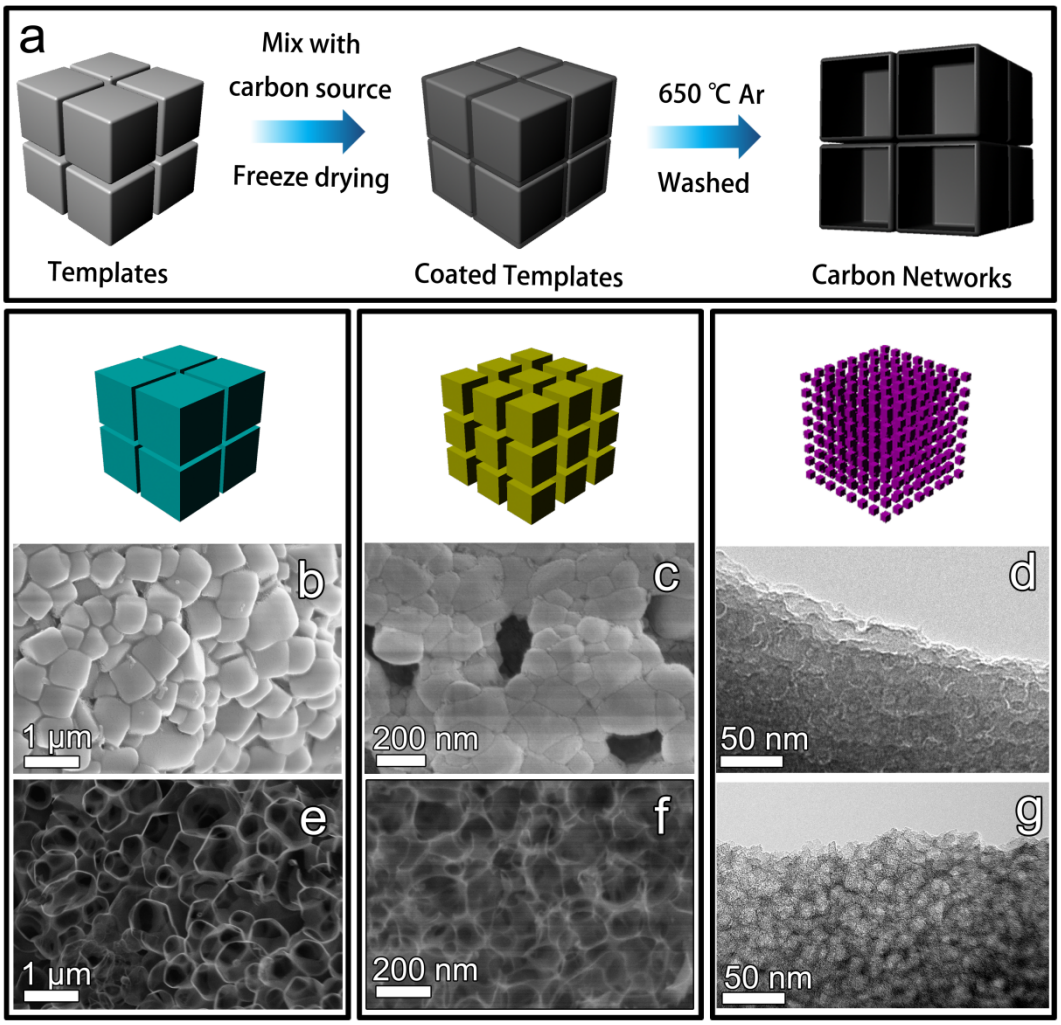

Fig. S3. (a) Synthesis scheme for the in-situ template method. SEM image of (b) carbon coated micro-sized NaCl and (c) carbon coated Na_2CO_3 with several hundreds of nanometers, (d) TEM image of carbon coated nano-sized Na_2SiO_3. After washing step, carbon networks with different pore sizes were obtained: SEM images of (e) HPC-B and (f) HPC-M; (g) TEM image of HPC-S.

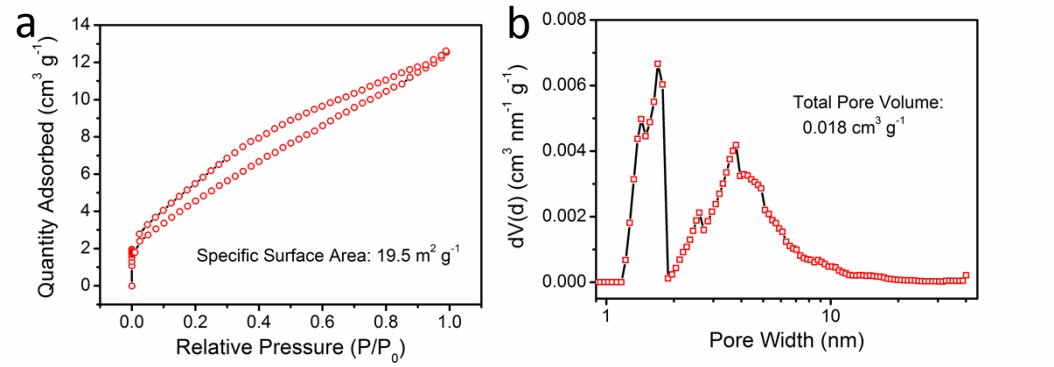

Fig. S4. (a) Adsorption-desorption isotherm and (b) the pore size distribution (PSD) of CB. According to the relevant report [S1], such micropores are derived from the pyrolysis of glucose. To further examine the origin of micropores in our case, the pore size distribution of CB was tested and plotted in Fig. S4. In the PSD result, the existence of micropores can be demonstrated, which

consolidate the assumption that the micropores come from glucose pyrolysis. In the fabrication process of HPC, the glucose located in the gap among salt template after freeze-drying or coated at the surface of salt as ultrathin layer. Moreover, such existence conditions enable the micropores developing comprehensively, and result in a high pore volume of HPCs.

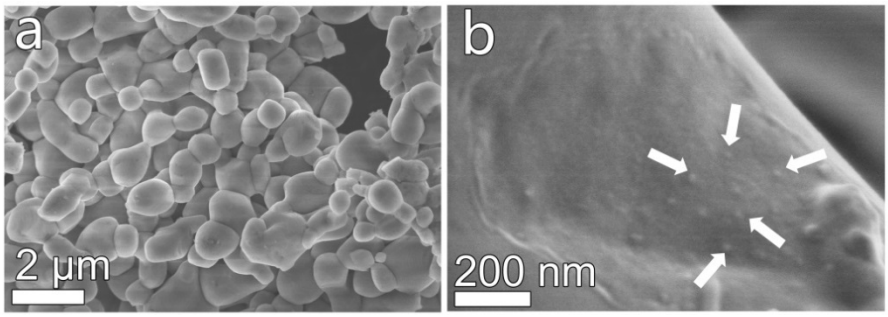

Fig. S5. SEM images of coated dual templates (before washing step) of HPC-BS: (a) NaCl particles and (b) nano-sized Na_2SiO_3 particles (indicated with white arrows) located on the surface of micro-sized NaCl particles.

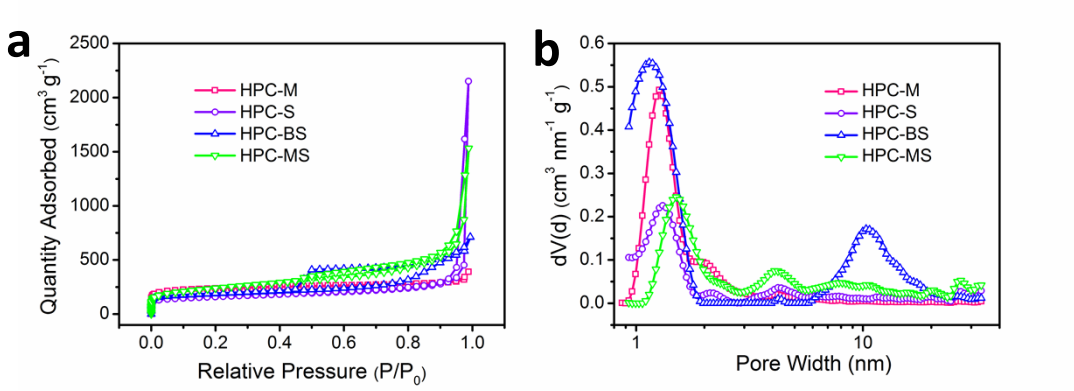

Fig. S6. (a) Adsorption-desorption isotherms and (b) pore size distributions of HPC-M, -S, -BS and -MS.

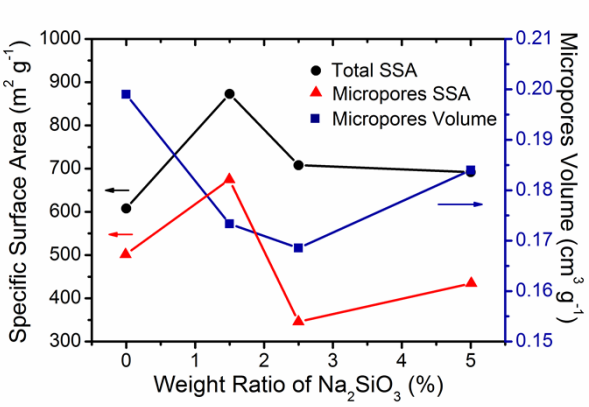

Fig. S7. Total SSA, micropores SSA, and micropores volume of HPC-BS at different salts ratio.

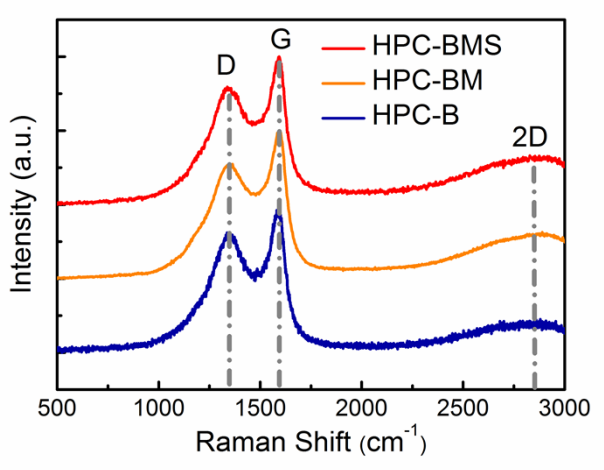

Fig. S8. Raman spectra of HPC-B, HPC-BM, and HPC-BMS.

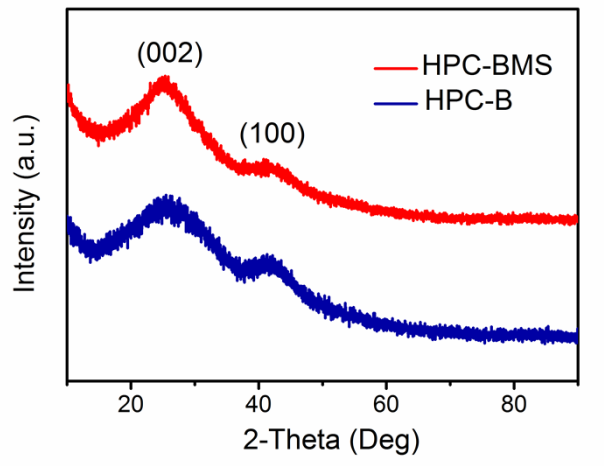

Fig. S9. XRD patterns of HPC-B and HPC-BMS.

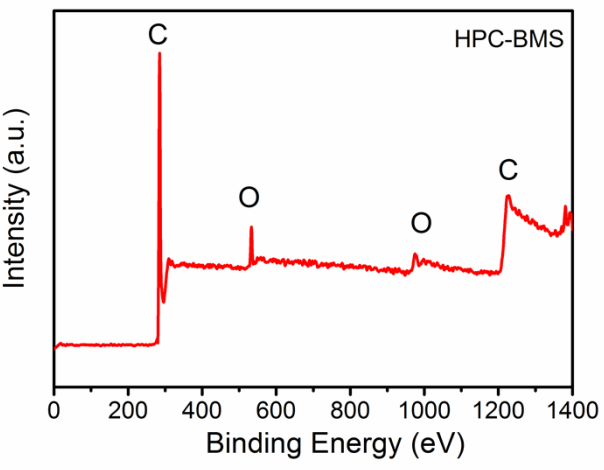

Fig. S10. X-ray photoelectron spectroscopy of HPC-BMS.

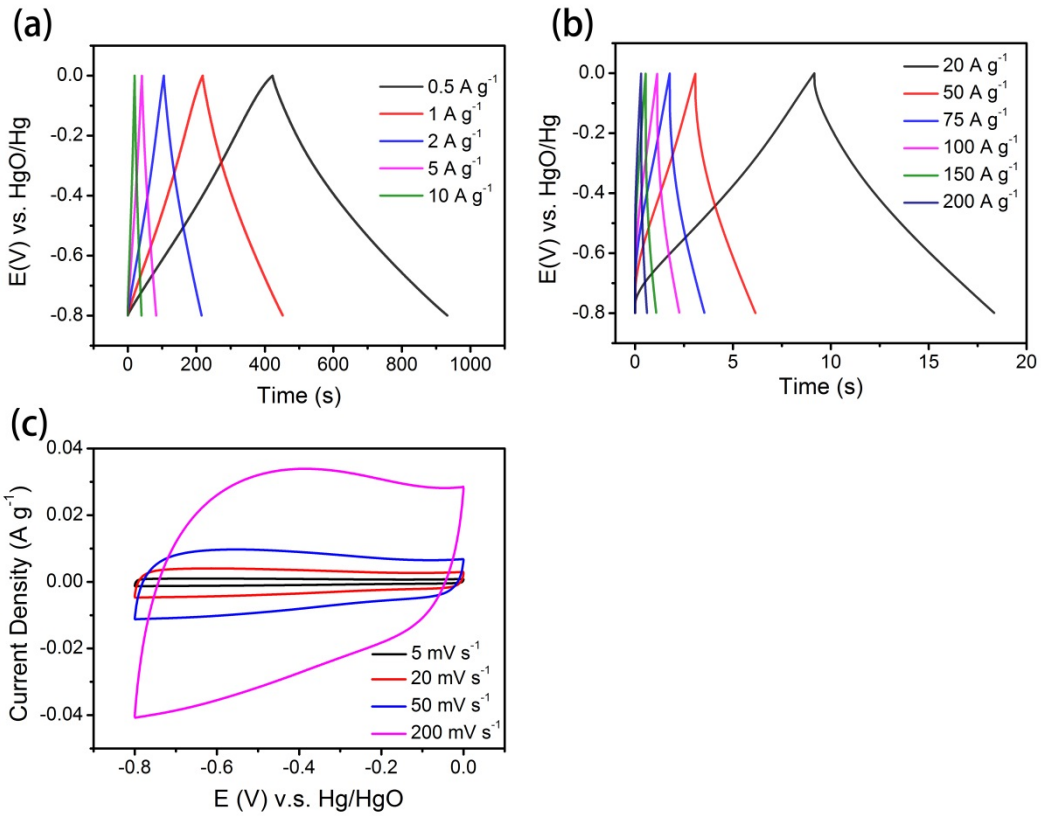

Fig. S11. (a) Electrochemical performance of HPC-BMS measured in a three-electrode system. (a) Charge-discharge curves at different current densities of 0.5, 1, 2, 5, and 10 A g^{-1}. (b) Charge-discharge curves at different current densities of 20, 50, 75, 100, 150, and 200 A g^{-1}. (c) CVs at scan rates of 5, 20, 50, and 200 mV s^{-1}.

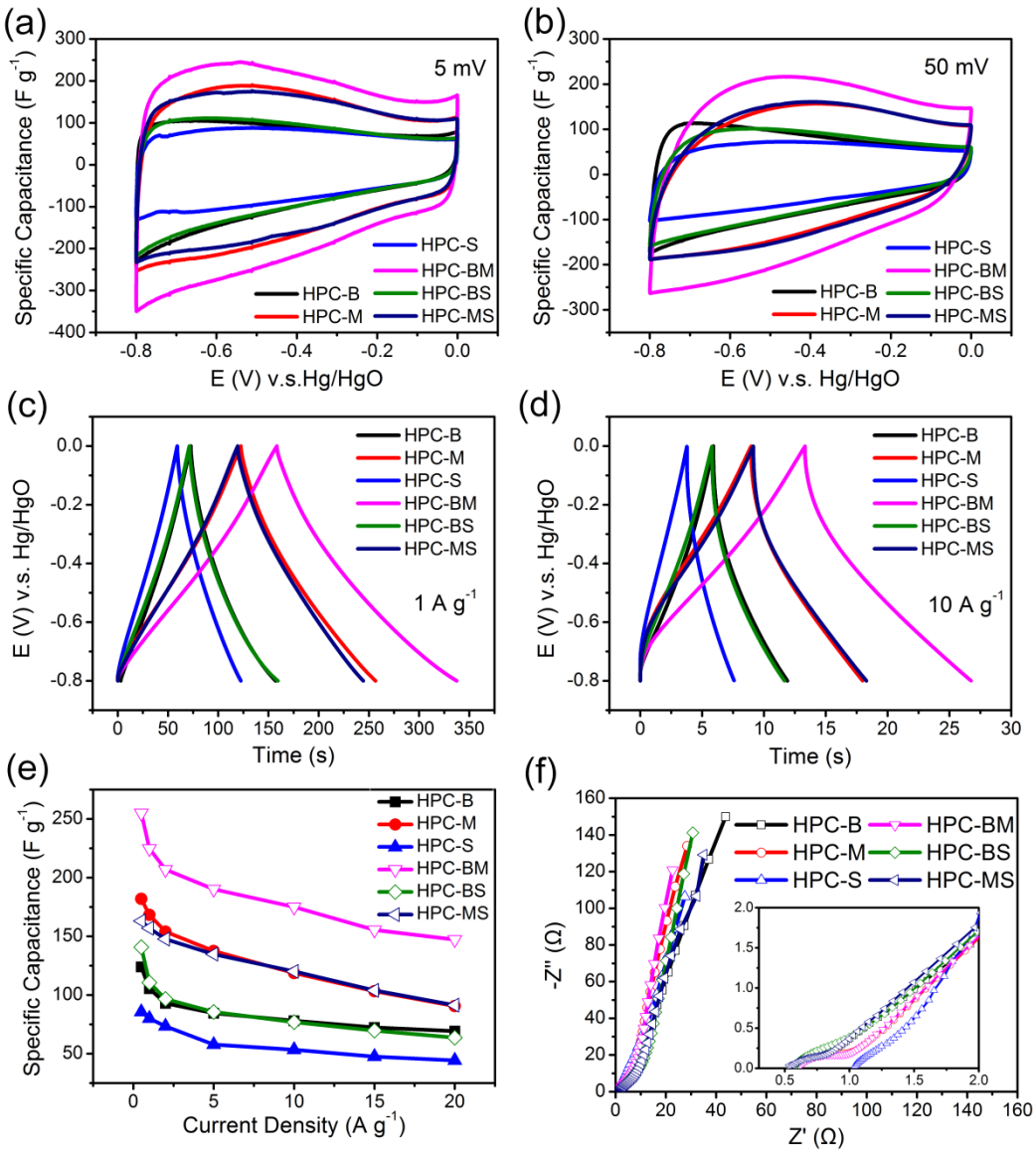

Fig. S12. Electrochemical performance of HPC-B, HPC-M, HPC-S, HPC-BM, HPC-BS and HPC-MS measured in a three-electrode system. CVs at a scan rate of (a) 5 mV s^{-1} and (b) 50 mV s^{-1}. Charge-discharge curves at different current densities of (c) 1 A g^{-1} and (d) 10 A g^{-1}. (e) Specific capacitances at different current densities, and (f) electrochemical impedance spectra.

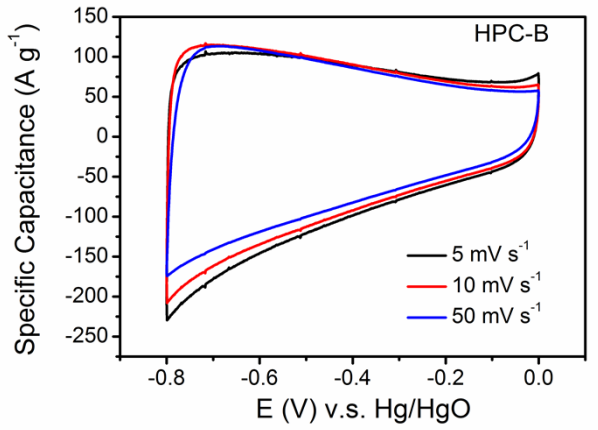

Fig. S13. CV curves of HPC-B at 5, 10, 50 mV s^{-1}

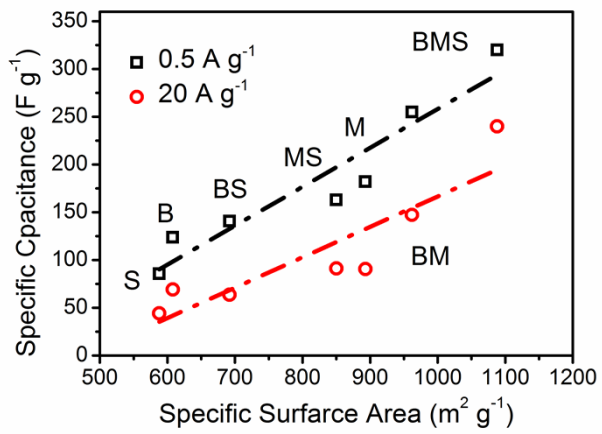

Fig. S14. The relationship between specific capacitances and specific surface areas.

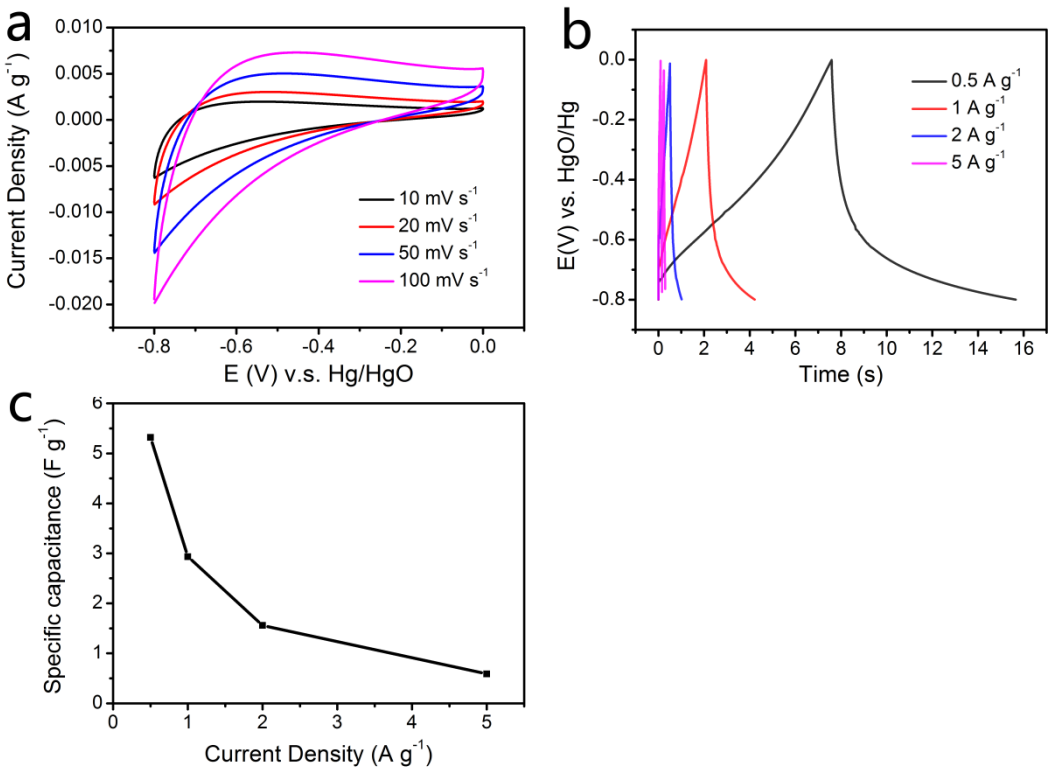

Fig. S15. Electrochemical performance of CB. (a) CV curves at different scan rates. (b) Charge-discharge curves and (c) specific capacitances at different current densities.

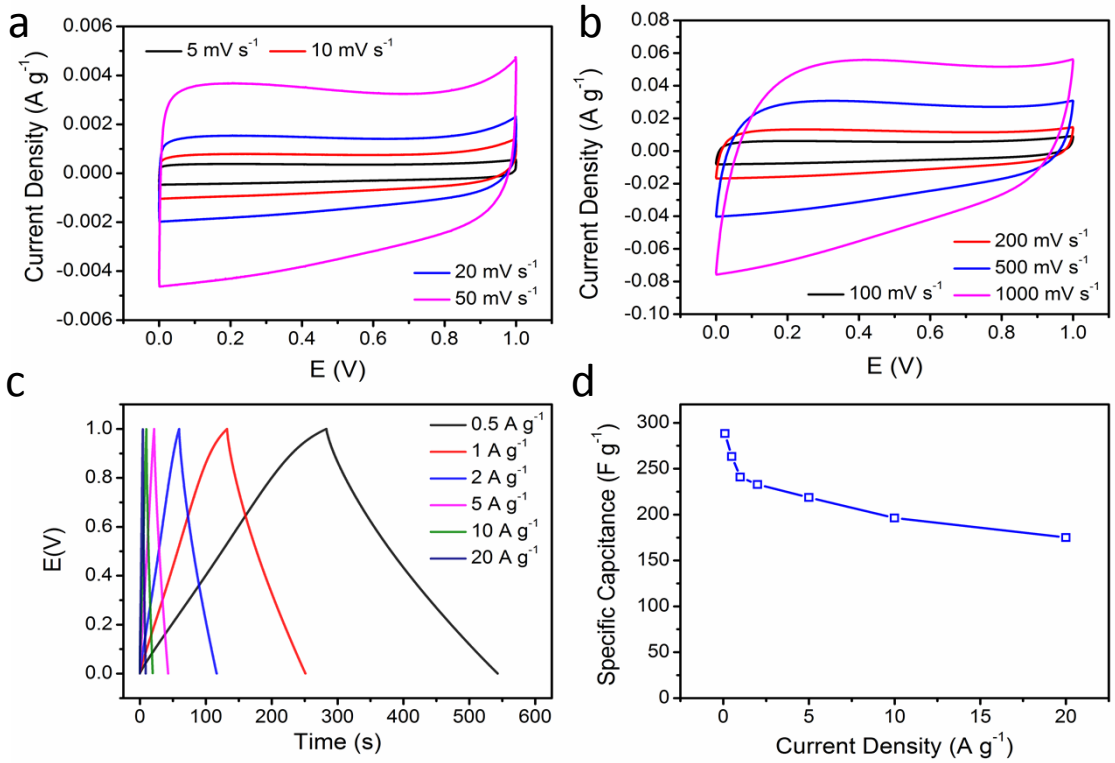

Fig. S16. Electrochemical performance of HPC-BMS in a two-electrode system. (a) CV curves at the scan rates from 5 to 50 mV s^{-1}. (b) CV curves at the scan rates from 100 to 1000 mV s^{-1}. (c) Charge-discharge curves and (d) specific capacitances at the current densities from 0.1 to 20 A g^{-1}.

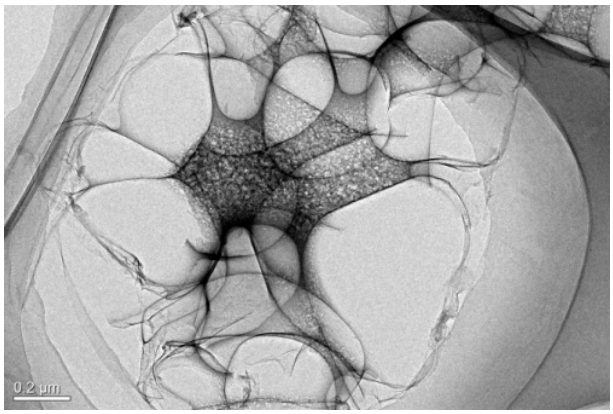

Fig. S17. TEM image of HPC-sw, in which dense distribution of mesopores can be observed.

References

[S1] S.-E. Chun, Y. Picard, J. F. Whitacre, *J. Eletrochem. Soc.*, 2011, **158**, A83-A92.